3. MUDELITE TÜÜBID

Kommentaare:

Reduktsionistlik tee	–	vt. eespool alamsüsteemid
Identifitseerimine	–	sisend - väljund signaalide analüüsis mudeli konstrueerimine

Üldnõuded mudelitele:

1. Paindlikkus (flexibility)
2. Kokkuhoidlikkus (parsimony)
   nn. Occhami printsiip
   miinimum arv vabu parameetreid/muutujaid
3. Võrdesindatus (equipresence)
   sõltuvad muutujad peaksid sõltuma
   kõigist sõltumatutest muutujatest (parameetritest)
4. Invariantsus (invariance)
   mudel ei tohi sõltuda koordinaatsüsteemi muutustest
5. Põhjus ja tagajärg (causality)

Põhitüübid:

1. Intuitiivsed ehk mõttelised
   - näiteks maailmavaade

2. Graafilised
   - merevee soolsus (näide)
   - peegelduskoefitsiendid (näide)
   - sumbuvuskoefitsiendid (näide)

3. Funktsionaalsed
   - DNA kaksikspiraal (näide)
   - membraan (näide)

4. Analüütilised

2. Graafilised

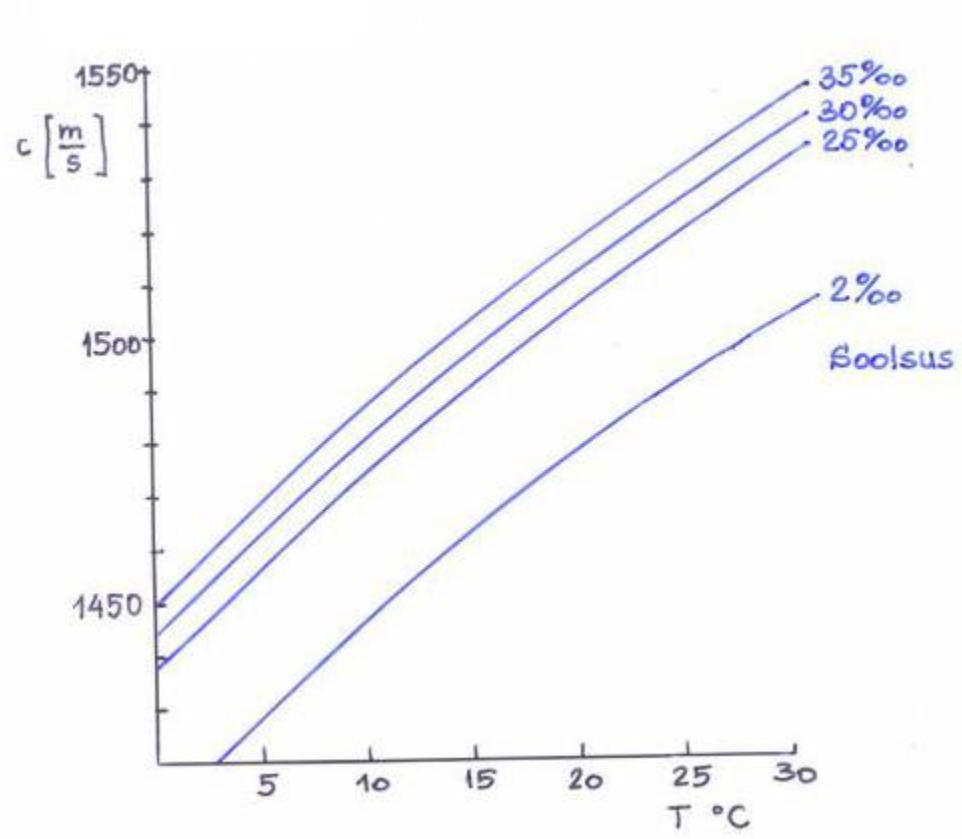

$c = 1448{,}96 + 4{,}591 - 5{,}304*10^{-2}T^2 + 2{,}37*10^{-4}T^3 + 1{,}3*4(S-35) + 1{,}63*10^{-2}D +$

$+ 1{,}675*10^{-7}D^2 - 1{,}025*10^{-2}T(S-35) - 7{,}139*10^{-13}T*D^3$

T – temperatuur, ^oC

S – soolsus, $^o/_{oo}$

D – sügavus, m

c – akustiliste lainete kiirus, m/s

3. Funktsionaalsed

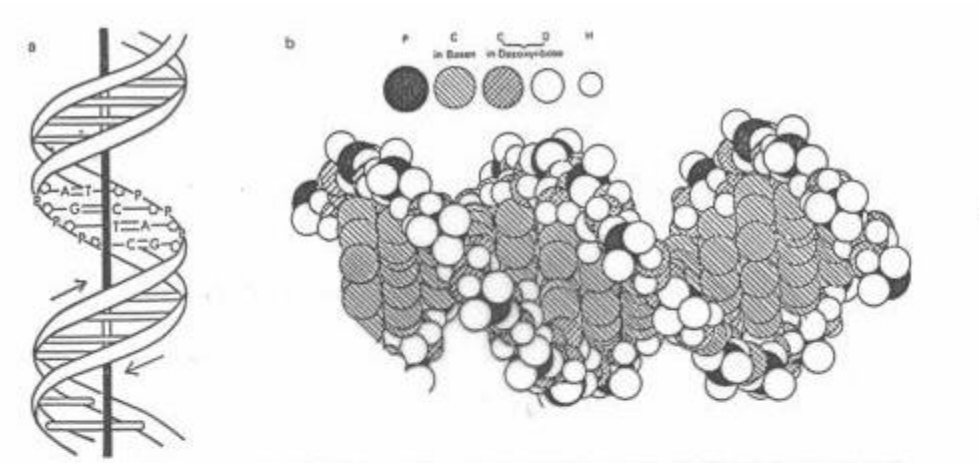

Abb. 2.10. (a) Schematische Darstellung der DNA-Doppelhelixstruktur (Typ B) mit antiparallelem Verlauf der komplementären 3'-P-5'-Phosphodiesterbindungen enthaltenden Polynucleotidstränge. (b) Kalotten-Modell der DNA-Struktur (Typ B) [nach Feugelman, M. et al.: Nature, Lond. 175, 834 (1955)]

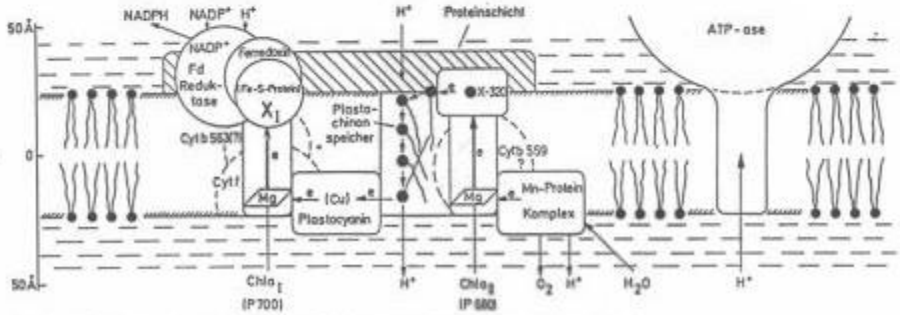

Abb. 13.15. Skizze des molekularen Aufbaues der Thylakoidmembran. (Nach Witt u. Mitarb., 1975)

4. Analüütilised

4.1. Staatilised → algebralised võrrandid
dünaamilised → diferents– või diferentsiaal-
võrrandid

Δt, t

"mälu" arvestamine

4.2. diskreetne aeg Δt
pidev aeg t

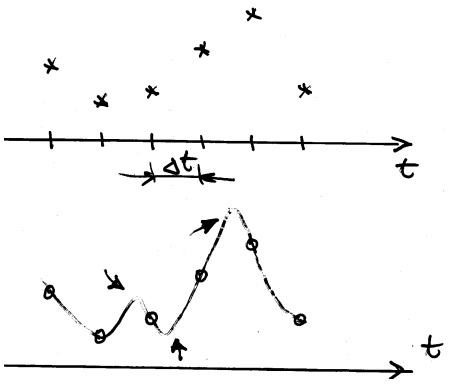

*mõõtmistulem või arvutuslikud tulemused

mõõtmised – diskreetselt
interpoleerimine?

diskreetne ruum Δx
pidev ruum x
vt. näide

diskreetne ruum + diskreetne aeg?
vt. rakuautomaadid

diskreetne ruum
kristallstruktuur
dislokatsioonid

Born-Karmani mudel

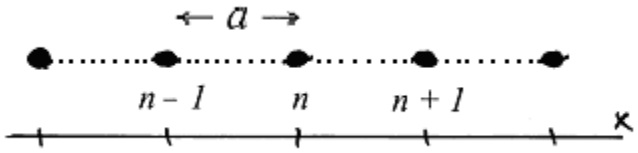

m – mass
k – vedru jäikus

algasend $x_n = na$
deformeerunud $x_n = na + U_n$, U_n – siire
liikumisvõrrand

$$m\frac{d^2U_n}{dt^2} = k(\xi_{n+1} - \xi_n), \quad \xi_n = U_n - U_{n-1}$$
$$= k(U_{n+1} - 2U_n + U_{n+1})$$

Taylori ritta:

$$U_{n\pm1} = U(x_n \pm a) \sim U(x_n) \pm \frac{\partial U}{\partial x}\Big|_{x_n} a + \frac{1}{2}\frac{\partial^2 U}{\partial x^2}\Big|_{x_n} a^2 + \ldots$$

asendades saame:

$U_{tt} - c_L^2 U_{xx} = 0$ hüperboolne 2. järku võrrand
lainevõrrand

$$c_L^2 = \frac{ka^2}{m} = \frac{E}{\rho_0}$$

$E = k/a$ elastsusmoodul

$\rho_0 = m/a^3$ tihedus

4.3. Sisend-väljund mudel

sisend — väljund — input – output
"must" kast — model

sisend — midagi on teada — väljund
hall
kast

Väljendus vorm:
diferents- või diferentsiaalvõrrand

<u>Triikraud</u>

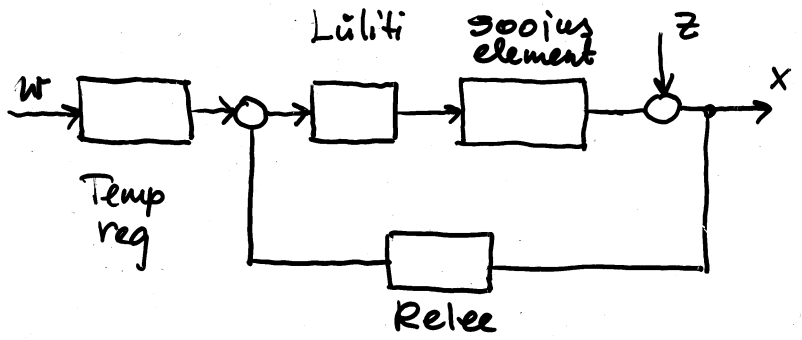

x – reguleeritav signaal, s.o. temperatuur
w – soovitud temperatuur
z – müra signaal, s.o. keskkonna temperatuuri erinevus

$$x=f(w,z)$$

4.4. Lineaarsed, mittelineaarsed

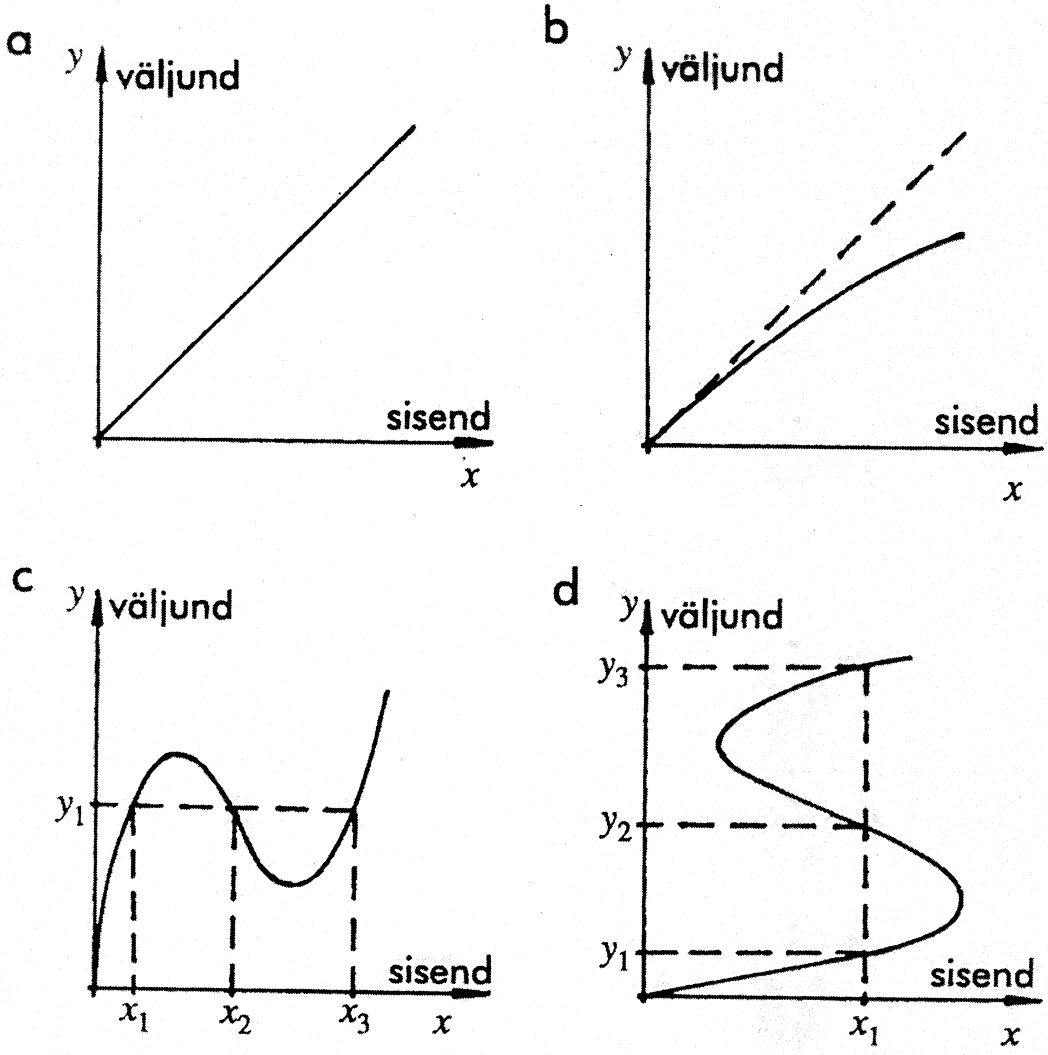

Sisendid ja väljundid lineaarsete ja mittelineaarsete funktsioonide puhul.

4.5. deterministlikud (määratud)
stohastilised (juhuslikud)

Kõik parameetrid määratud – deterministlik

juhuslikud suurused (parameetrid) – stohastiline

Kui oluline iseärasus

Mittelineaarne mudel	Determineeritud	Stohastiline
Tulemus	determi-neeritud kaootiline	stohastiline
Erinevus:	K = 0 K = lõplik arv	K = ∞

K – Kolmogorovi entroopia

Täpsemalt kursuses "Mittelineaarne dünaamika ja kaos"

4.6. Jaotatud parameetritega mudel
koondatud parameetritega mudel

Koondatud – lõplik arv diferents – või harilikke diferentsiaal võrrandeid

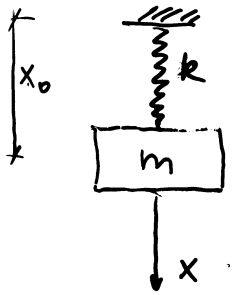

m - mass
k - vedru jäikus

$m\ddot{x} = mg - k(x_0 + x)$

$mg = kx_0$

$m\ddot{x} + kx = 0$

Jaotatud – osatuletistega diferentsiaalvõrrandid

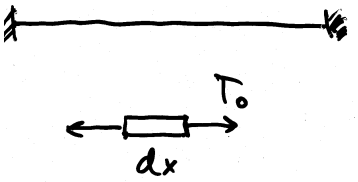

keel / string

T_0 – tõmme

ρ – tihedus

põikisiire – u

$$T_0 \frac{\partial^2 u}{\partial x^2} = \rho \frac{\partial^2 u}{\partial t^2}$$

$$u_{tt} - c^2 u_{xx} = 0$$

hüperboolne
laine võrrand

$$c^2 = \frac{T_0}{\rho}$$

Tänapäeval oluline ka hübriidmudel jaotatud + koondatud parameetrid

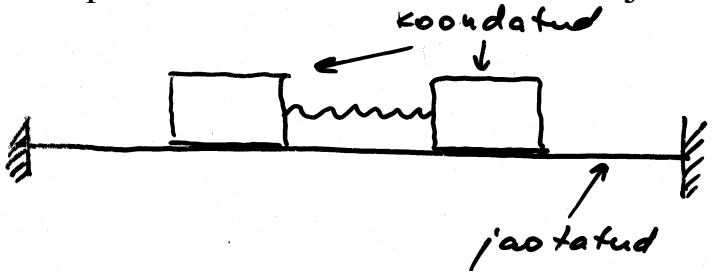

multi – body dynamics
süsteemidünaamika

Näide: kristallstruktuur
üleminek diskreetselt pidevale

4.7 aeg – invariantsed mudelid
ajast sõltuvad mudelid

time – invariant
time – varying

4.8 loogilis – hierarhilised mudelid

Vt. A. Merilai Kõneaktide teooria
Akadeemia, 1998, 10, N 11, 2263-2298

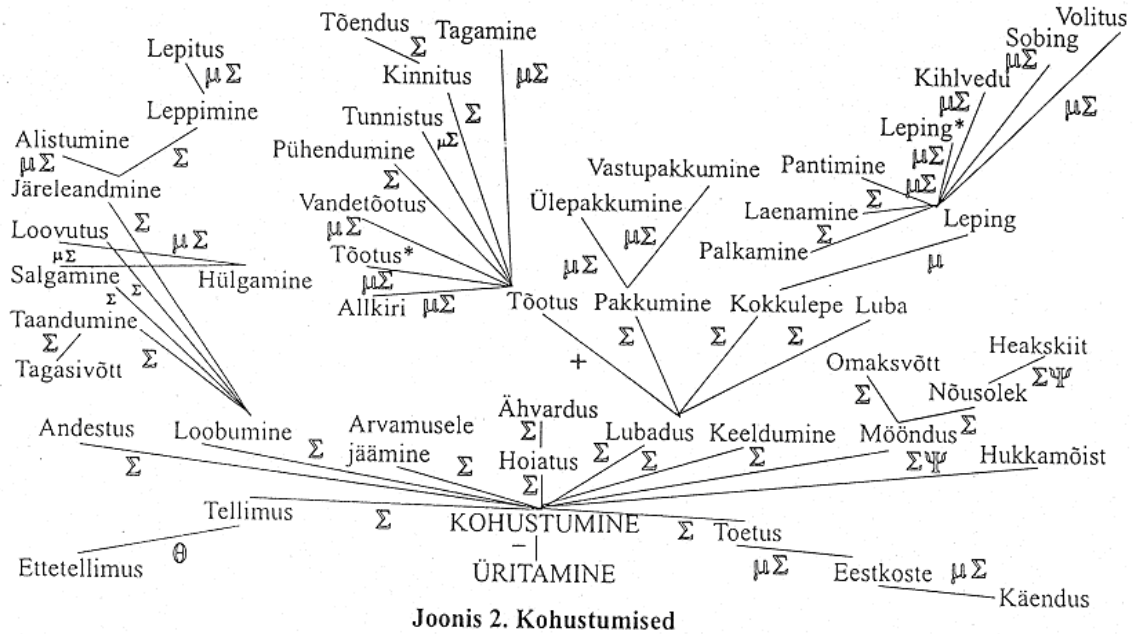

Joonis 2. Kohustumised

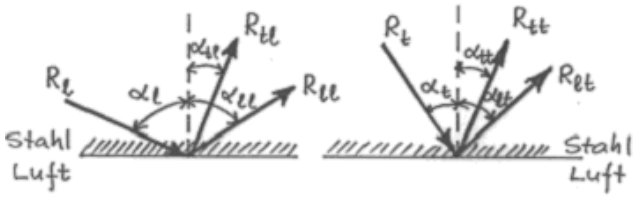

Tafel 1. Reflexionsfaktoren bei freier Grenzfläche von Stahl

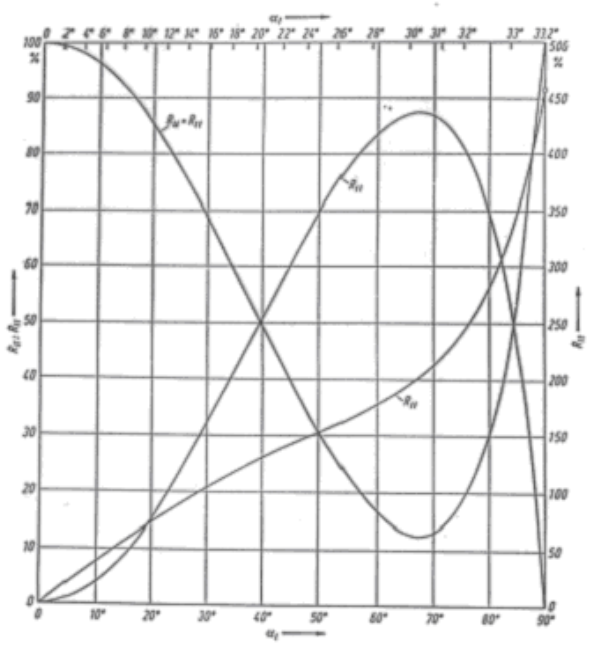

Tafel 10. Schwächung einer ebenen Welle

Verschiedene Schwächungskoeffizienten und Schichtdicken nach Formel $p/p_0 = e^{-\alpha d}$. Rechte Skala Schwächung in dB, linke Skala rel. Schalldruckamplitude bzw. Echohöhe in Prozent

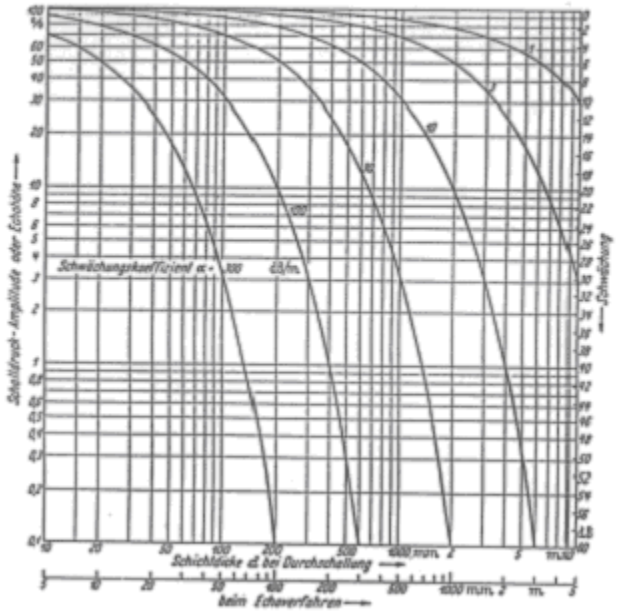

Lainete peegeldus

LINEAR → **NONLINEAR**

täpsustamine
perturbations

NONLINEAR → **LINEAR**

lihtsustamine
approximations

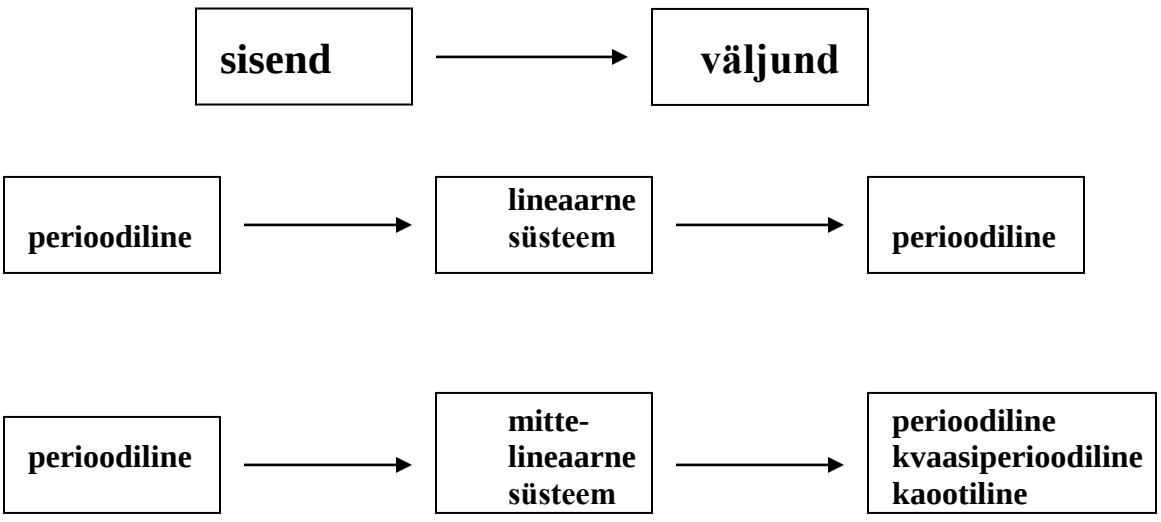

Mittelineaarsus

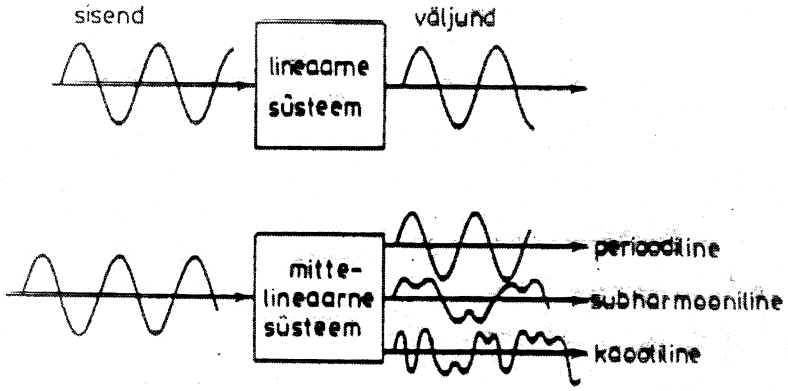

Lineaarse ja mittelineaarse süsteemi väljundite erinevus.
Moon, 1987.

Duffingi võrrand

$$\ddot{x} + a\dot{x} + bx + cx^3 = f\cos\omega t$$

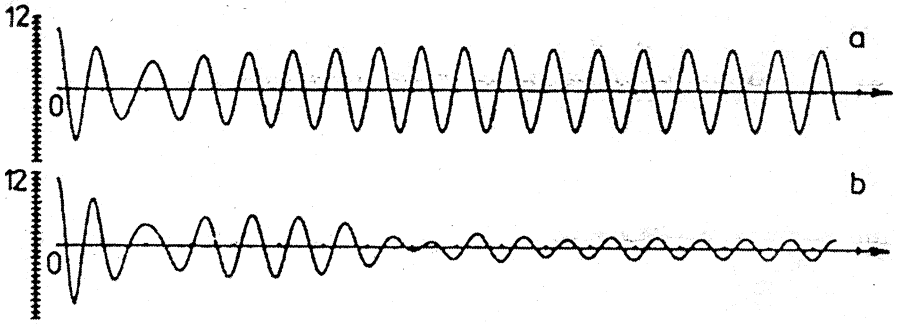

Mittelineaarse sumbuva sundvõnkumise graafik:
(a) $x_{01} = A,\ \dot{x}_{01} = 0$;
(b) $x_{02} = B,\ \dot{x}_{02} = 0,\ A < B$; väiksem algamplituud tekitab suurema amplituudiga võnkumise.
Thompson, Stewart, 1986.

Näide 1. Rakuenergeetika

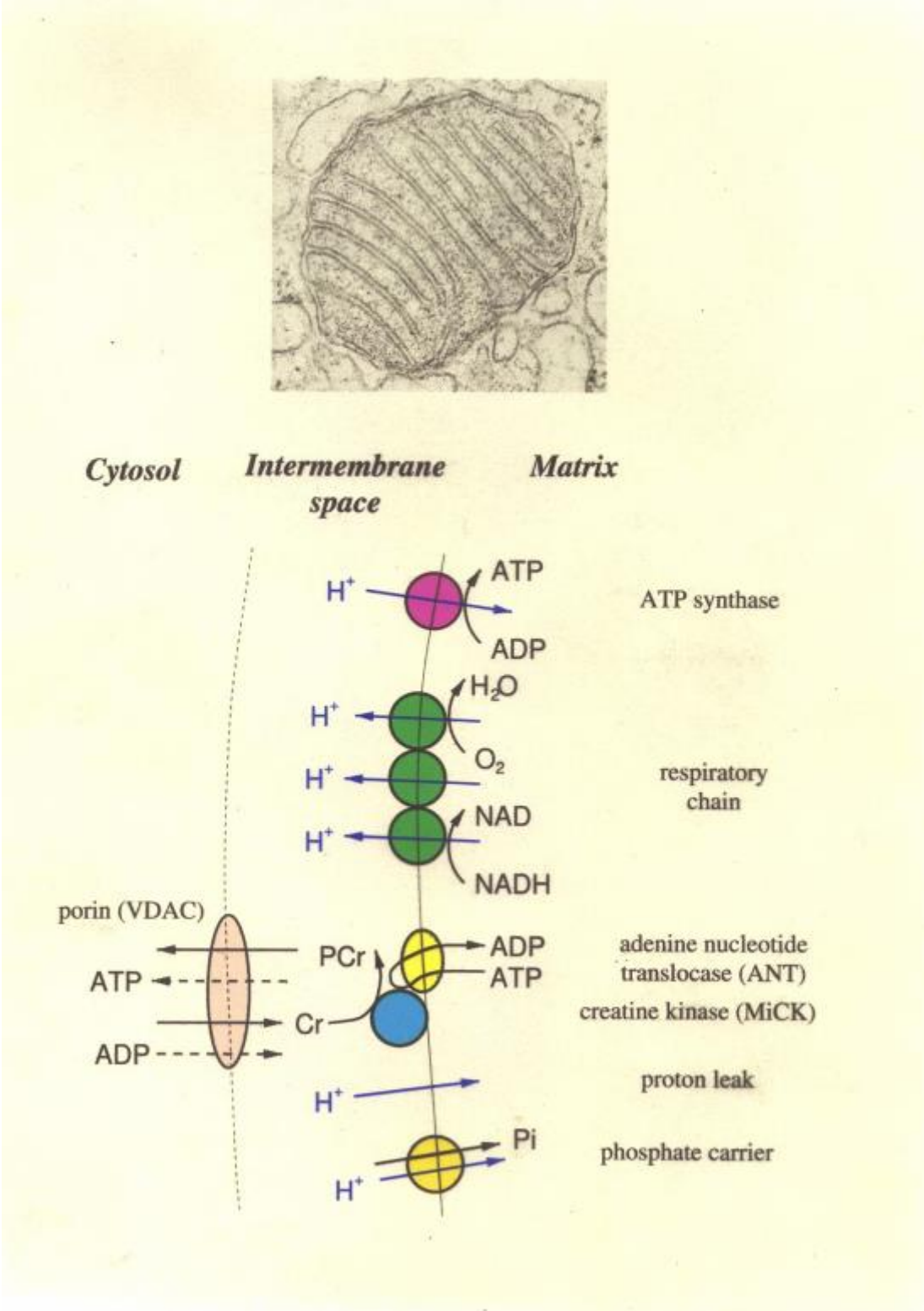

Danger No. 1: Calcium Overload and Mitochondrial Permeability Transition

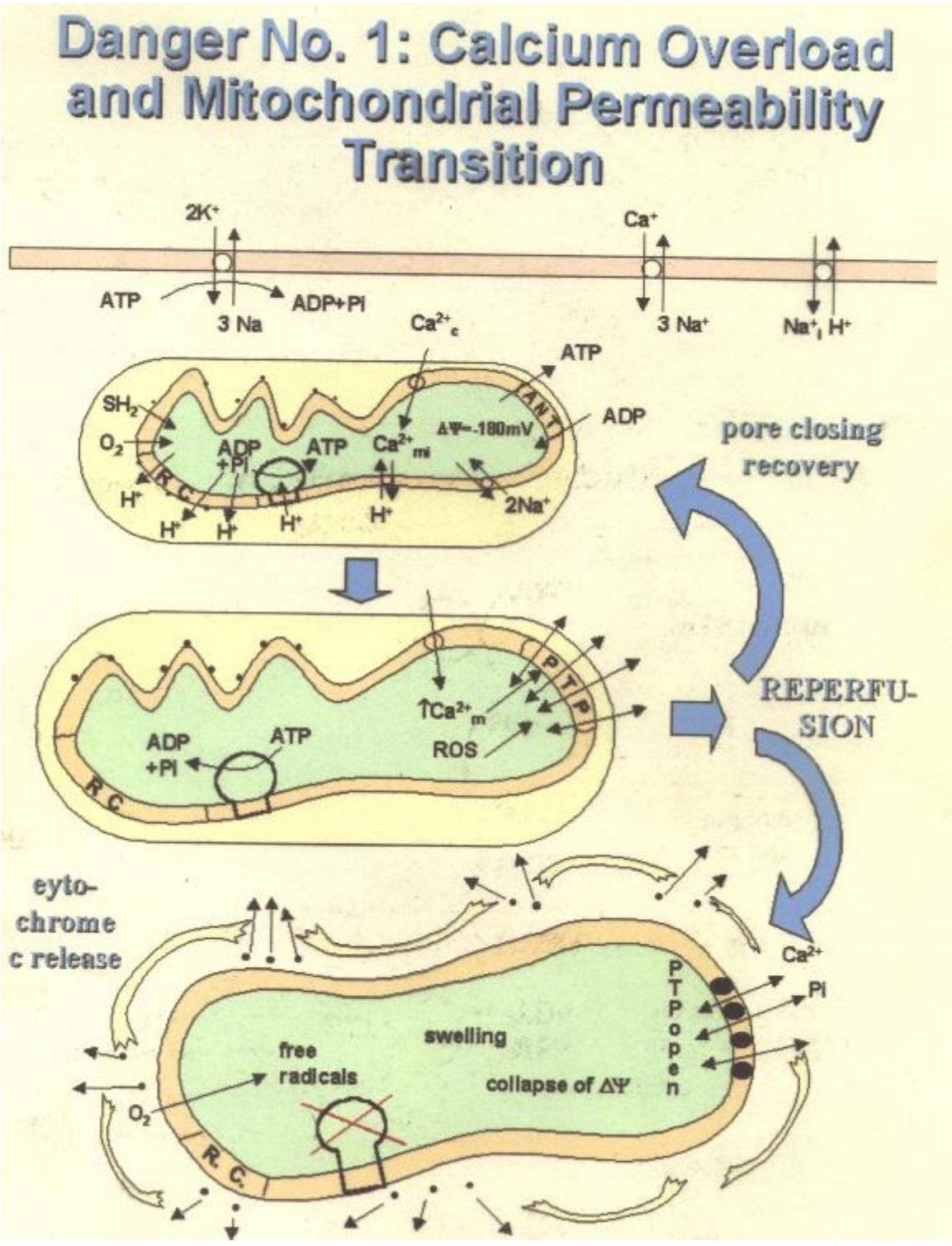

Näide 2. Rakuautomaadid (Cellular automata)

Rakuautomaat: elementide (rakkude) kogum, mille omaduste muutmiseks rakendatakse teatud reeglite kogum

Ruum: diskreetne (1D, 2D, 3D)

Aeg: diskreetne

Olulised viited:

1. Stephen Wolfram A New Kind of Science. Wolfram Media, Champaigne (Illinois), 2002
   (S. Wolfram is the author of Mathematica, www.stephenwolfram.com)
2. Daniel T. Kaplan. Nonlinear Dynamics in Cardiac Conduction, In A.S. Perelson et al (eds.), Nonlinearity in Biology and Medicine. Elsevier, New York, 1988, 19-49

Joonised:

1. Kristallstruktuurid
2. Rakuautomaatide idee S.Wolframi näidetest
3. 3. Erutusfrondi levi südamelihases D.Kaplani jt. näidetes

The sequence of 256 possible cellular automaton rules of the kind shown above. As indicated, the rules can conveniently be numbered from 0 to 255. The number assigned is such that when written in base 2, it gives a sequence of 0's and 1's that correspond to the sequence of new colors chosen for each of the eight possible cases covered by the rule.

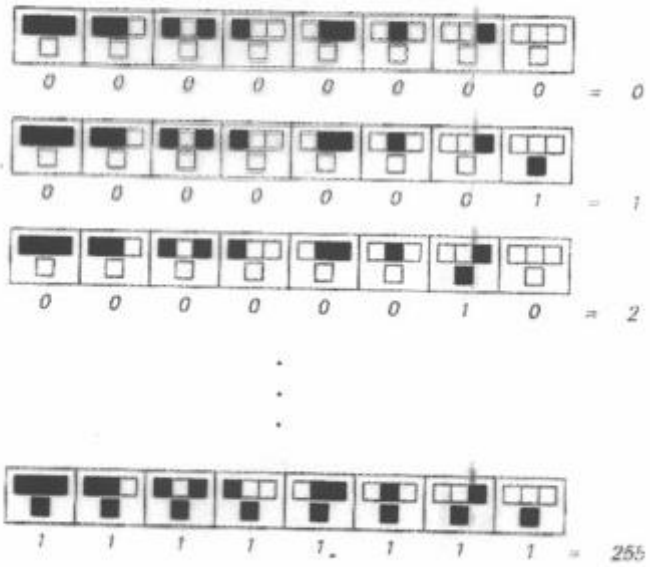

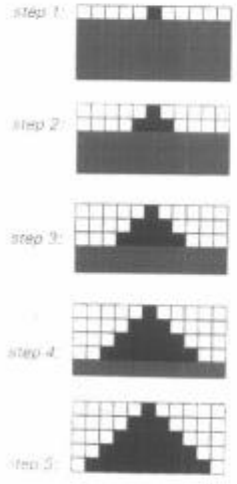

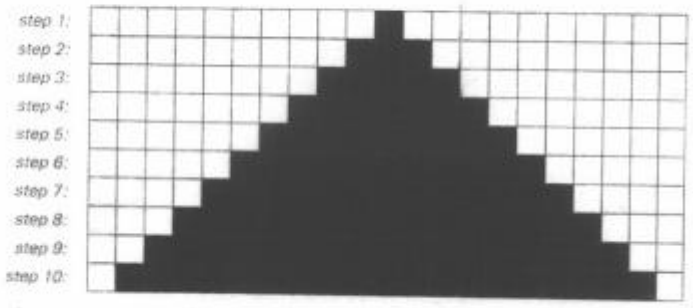

A visual representation of the behavior of a cellular automaton, with each row of cells corresponding to one step. At the first step the cell in the center is black and all other cells are white. Then on each successive step, a particular cell is made black whenever it or either of its neighbors were black on the step before. As the picture shows, this leads to a simple expanding pattern uniformly filled with black.

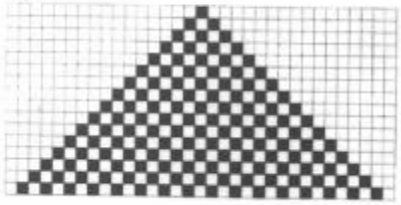

A cellular automaton with a slightly different rule. The rule makes a particular cell black if either of its neighbors was black on the step before, and makes the cell white if both its neighbors were white. Starting from a single black cell, this rule leads to a checkerboard pattern. In the numbering scheme of Chapter 3, this is cellular automaton rule 250.

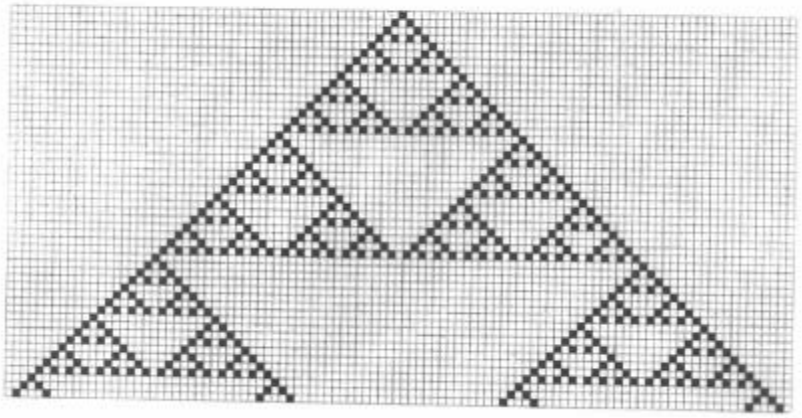

A cellular automaton that produces an intricate nested pattern. The rule in this case is that a cell should be black whenever one or the other, but not both, of its neighbors were black on the step before. Even though the rule is very simple, the picture shows that the overall pattern obtained over the course of 50 steps starting from a single black cell is not so simple. The particular rule used here can be described by the formula $a'_i = Mod[a_{i-1} + a_{i+1}, 2]$. In the numbering scheme of Chapter 3, it is cellular automaton rule 90.

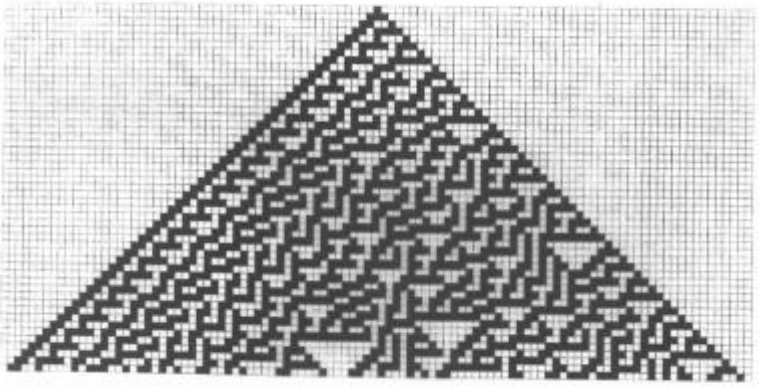

A cellular automaton with a simple rule that generates a pattern which seems in many respects random. The rule used is of the same type as in the previous examples, and the cellular automaton is again started from a single black cell. But now the pattern that is obtained is highly complex, and shows almost no overall regularity. This picture is our first example of the fundamental phenomenon that even with simple underlying rules and simple initial conditions, it is possible to produce behavior of great complexity. In the numbering scheme of Chapter 3, the cellular automaton shown here is rule 30.

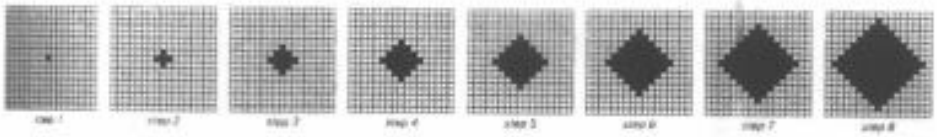

Successive steps in the evolution of a two-dimensional cellular automaton whose rule specifies that a particular cell should become black if any of its neighbors were black on the previous step. (In the numbering scheme described on page 173 this rule is code 1022.)

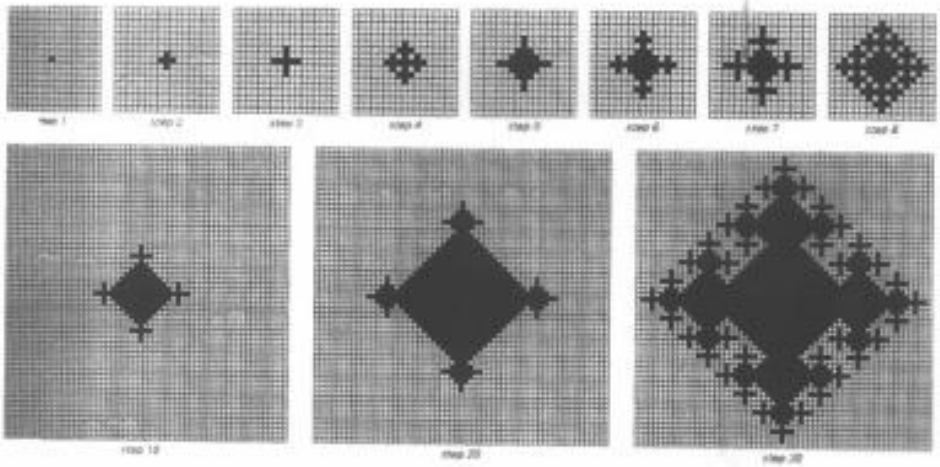

Steps in the evolution of a two-dimensional cellular automaton whose rule specifies that a particular cell should become black if exactly one or all four of its neighbors were black on the previous step, but should otherwise stay the same color. Starting with a single black cell, this rule yields an intricate, if very regular, pattern of growth. (In the numbering scheme on page 173, the rule is code 942.)

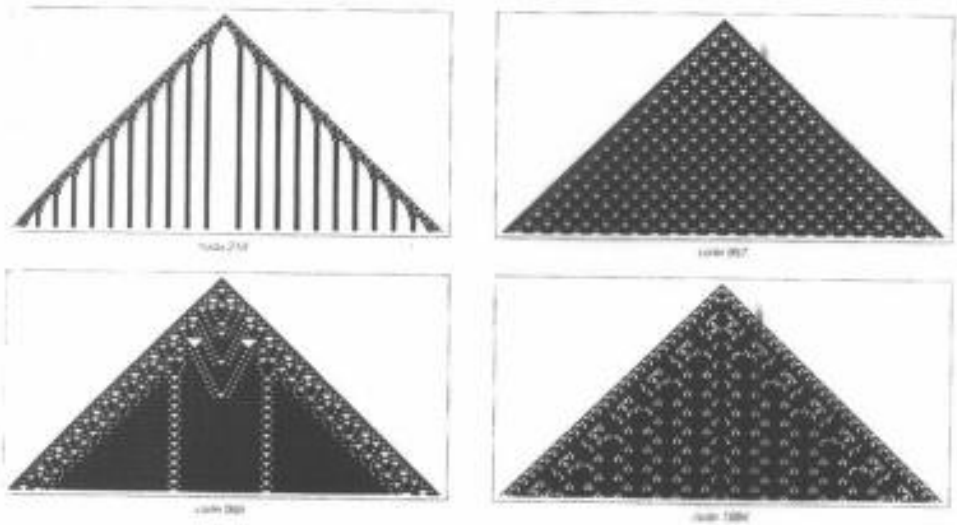

Examples of three-color totalistic rules that yield patterns which grow forever but have a fundamentally repetitive structure.

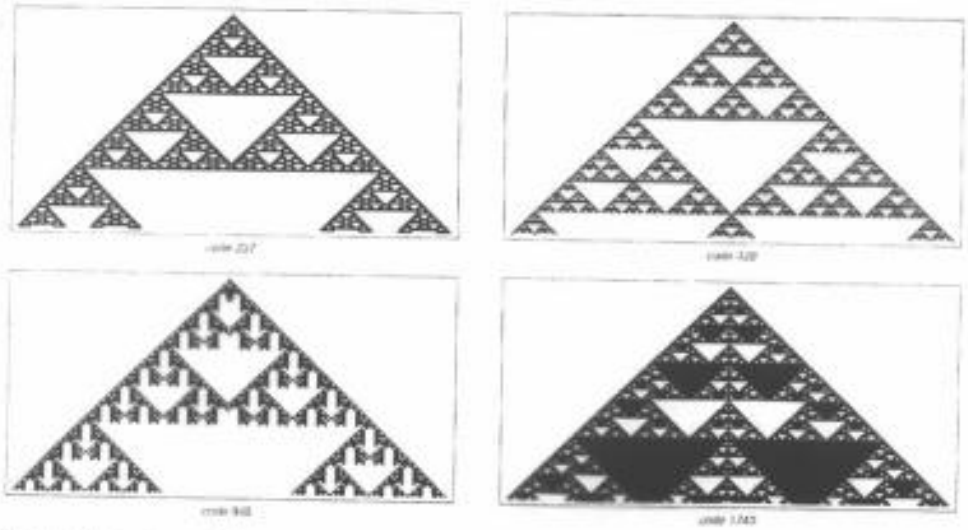

Examples of three-color totalistic rules which yield nested patterns. In most cases, these patterns have an overall form that is similar to what was found with two-color rules. But code 420, for example, yields a pattern with a slightly different structure.

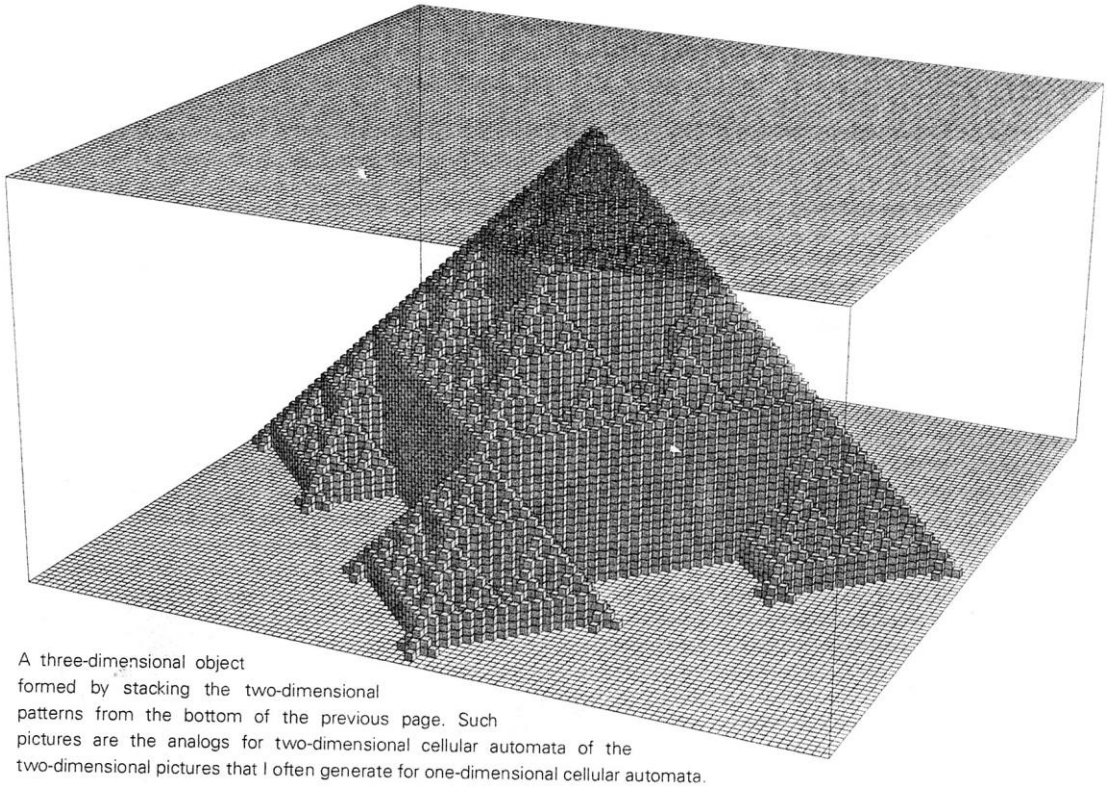

A three-dimensional object formed by stacking the two-dimensional patterns from the bottom of the previous page. Such pictures are the analogs for two-dimensional cellular automata of the two-dimensional pictures that I often generate for one-dimensional cellular automata.

Näide 3. Erutusfrondi levi südamelihases D.Kaplani jt. näidetes

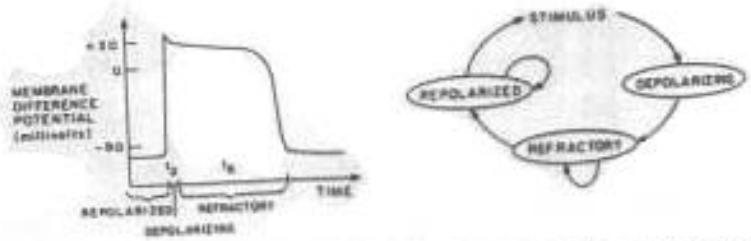

FIG. 3. (a) A schematic drawing of the transmembrane electrical potential of a heart cell during an action potential (total duration approx. 200 ms) is divided into sections corresponding to the communication states of the model. (b) A transition diagram showing the communication states of the model.

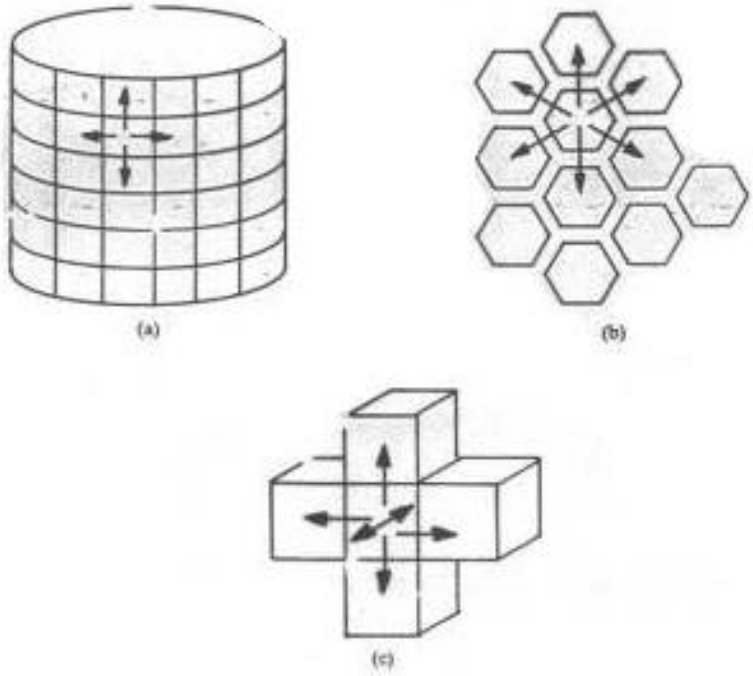

FIG. 4. The topology of neighbor-to-neighbor connections: (a) Each element has 4 neighbors on a cylinder. (b) Each element has 6 neighbors. A cylindrical version of this topology is used in the model which generated the illustrations for this paper. (c) A three-dimensional topology. Each element has 6 neighbors. Topologies with up to 26 neighbors per element have been used.

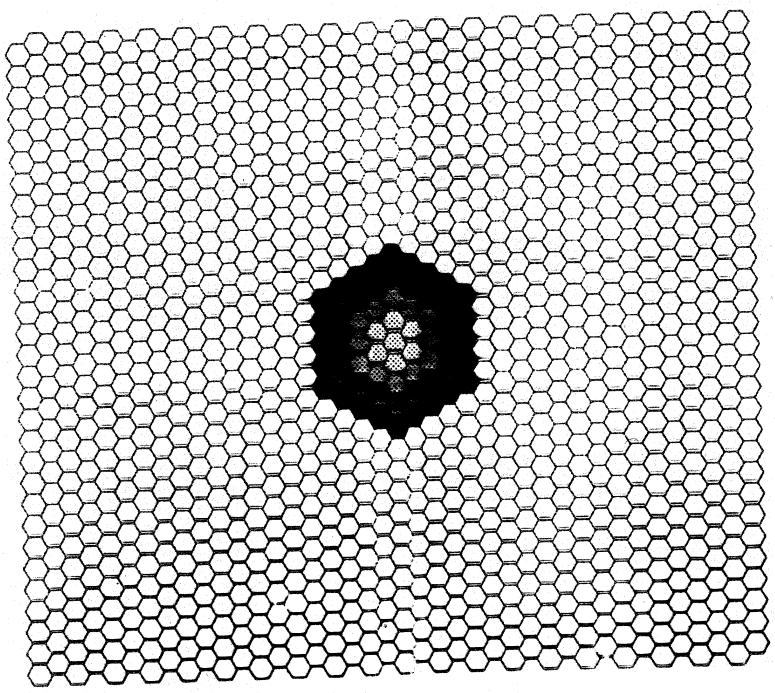

(a)

FIG. 5. The response to a single stimulus. Black: depolarizing (i.e. on the wavefront of activation). White: repolarized. Gray: depolarized (refractory); lighter elements are near the end of their refractory periods. (a) The wavefront spreads out from the site of stimulation (the center of the array). (b) The wave somewhat later than in (a); elements near the center have repolarized.

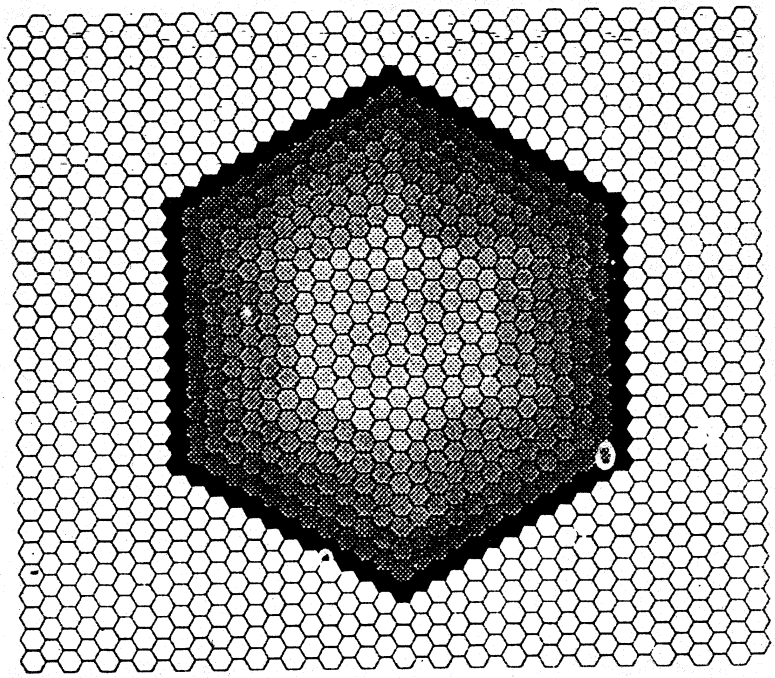

(b)

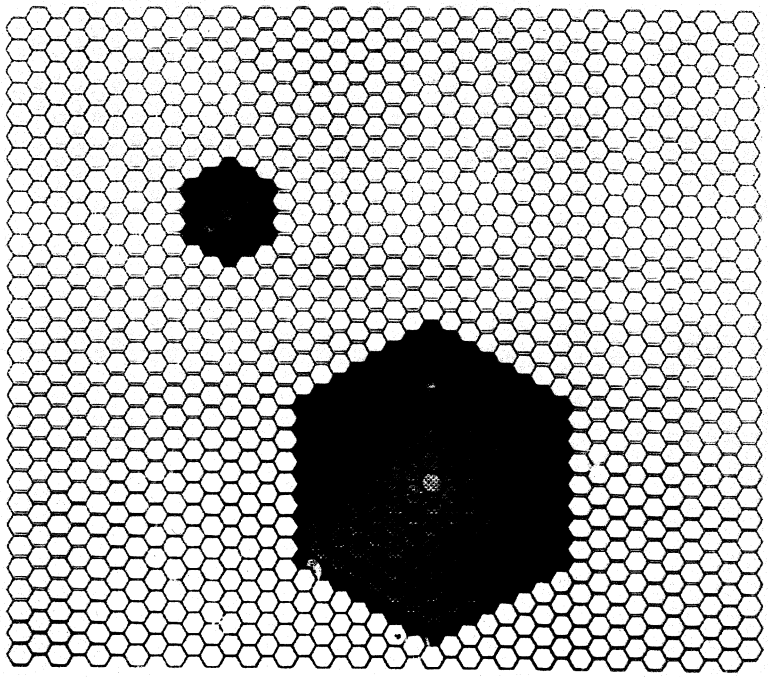

(a)

FIG. 6. (a) Two elements are stimulated in close succession, causing waves to spread out from the points of stimulation. (b) The wavefronts annihilate each other when they collide.

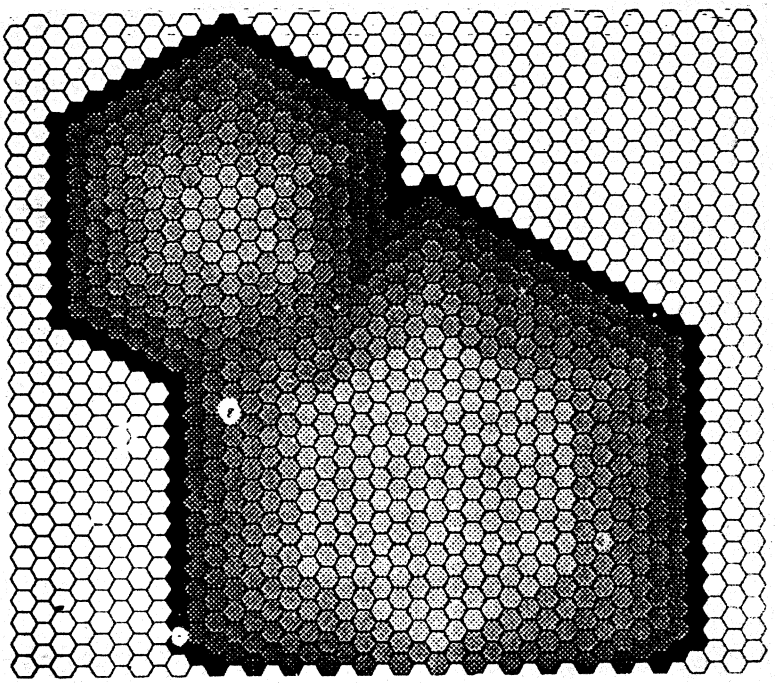

(b)

FIG. 6 (Continued)

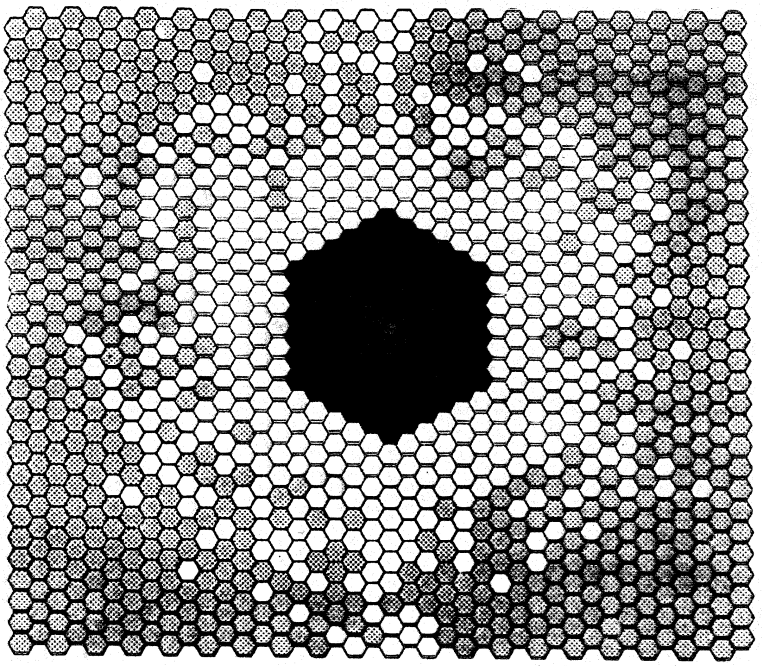

(a)

FIG. 7. The response to train of stimuli. (a) The elements near the outside of the array are refractory from the previous stimulation. The wavefront in the center propagates without running into refractory elements. (b) Stimuli were given in more rapid succession than in (a). The second wavefront runs into refractory elements.

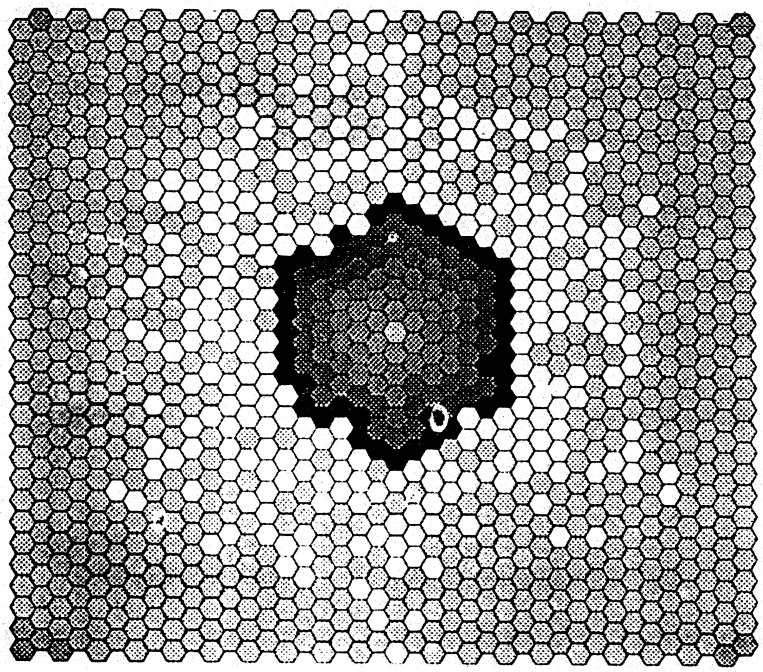

(b)

FIG. 7 (Continued)

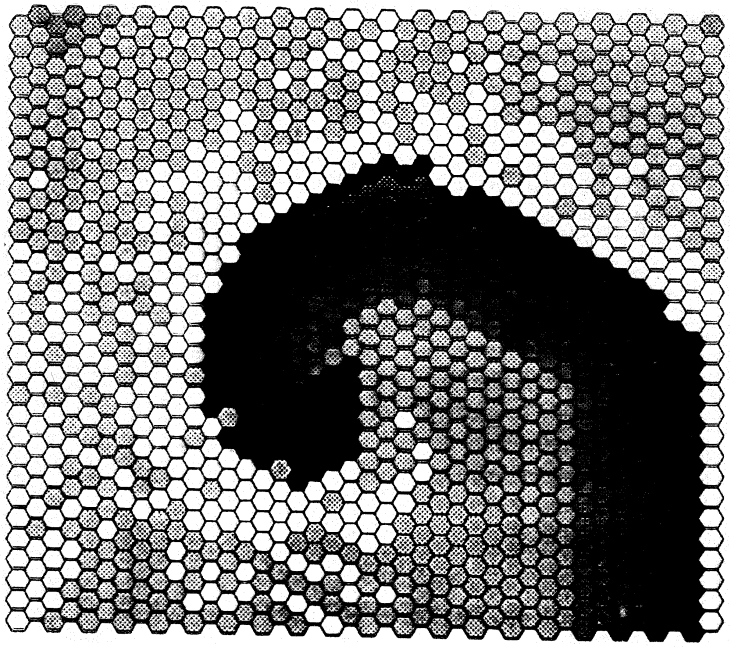

FIG. 12. A rotor in an inhomogeneous medium. The rotor's wavefront begins to fractionate. If inhomogeneities are large enough, further reentry may develop as in Figure 8. Although the mean refractory period is the same as in Figure 11, the rotor has slowed. This is evidenced by the appearance of greater numbers of repolarized elements than in Figure 11.

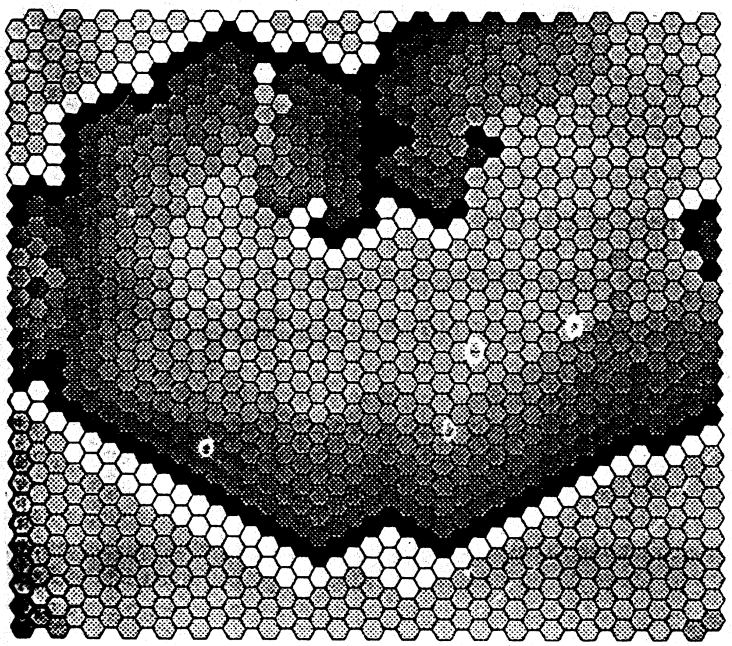

FIG. 13. The pattern which develops when the dispersion of refractoriness is removed from the fibrillating array shown in Figure 9. The simplified pattern that results can most easily be characterized as a pair of rotors.

Näide 4. Keemia

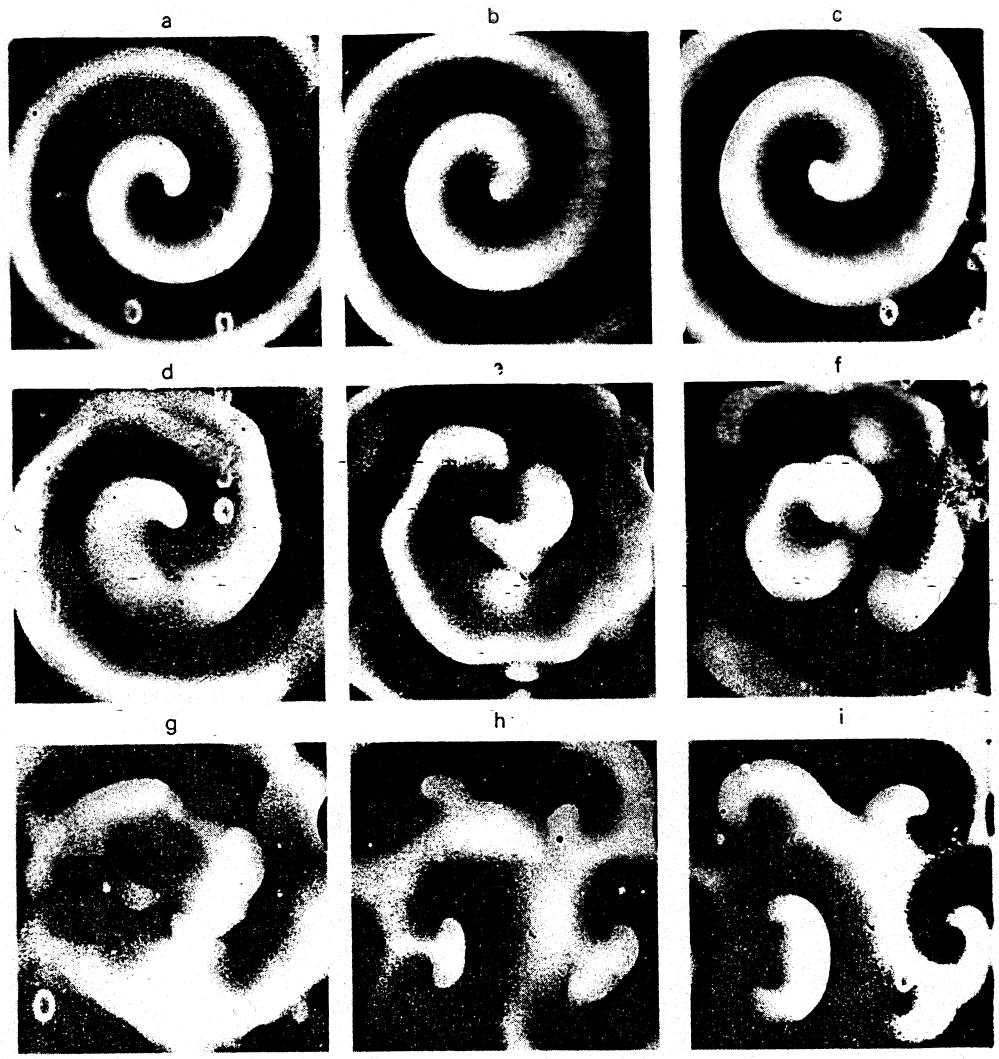

Fig. 1. Transition from order to disorder, and back to order for a spiral of the Belousov-Zhabotinskii reaction in a thin liquid layer.

Näide 5. Kolloidsed osakesed

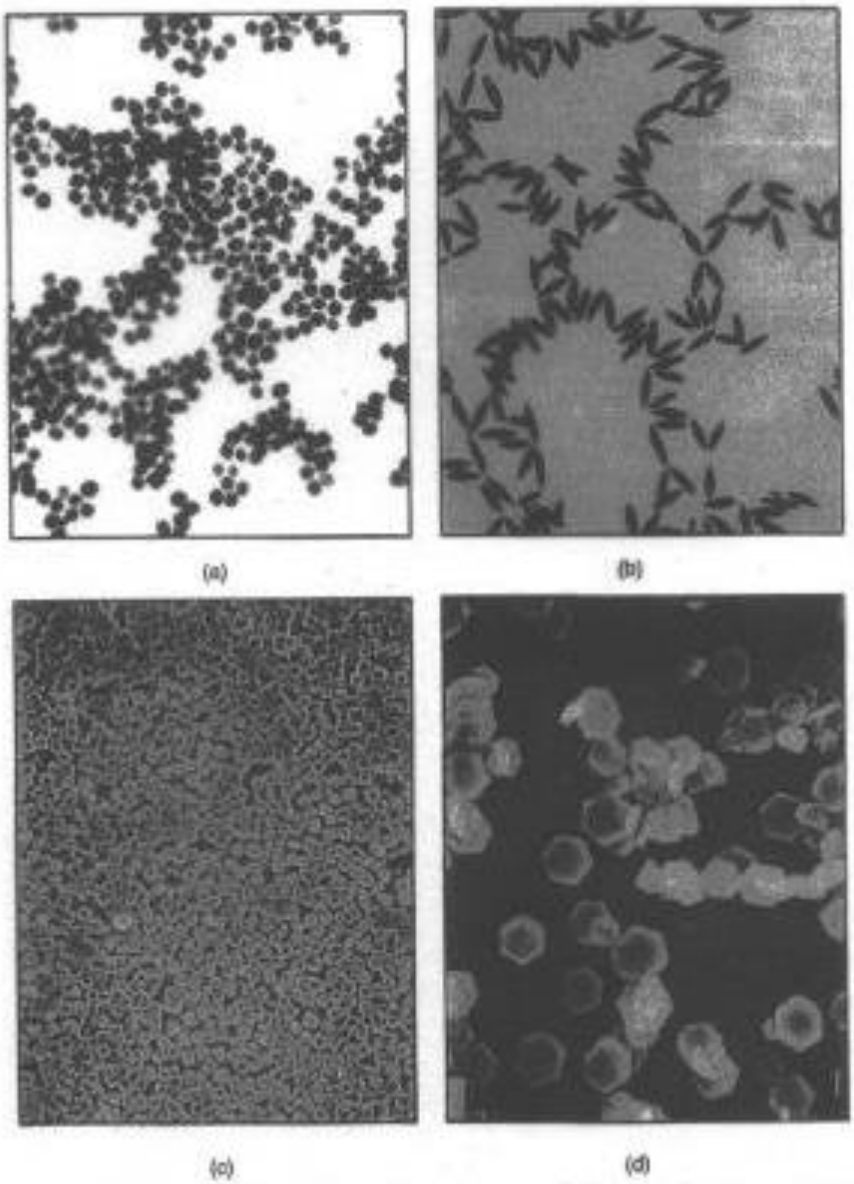

Figure 4.7. Colloidal α-Fe_2O_3 particles with various morphologies: (*a*) spheres; (*b*) spindles; (*c*) cubes; (*d*) hexagonal disks. Each bar indicates 2 μm. [From M. Ozaki, *Mater. Res. Soc. Bull.* (12), 35 (1989).]

Näide 6. Kristallid

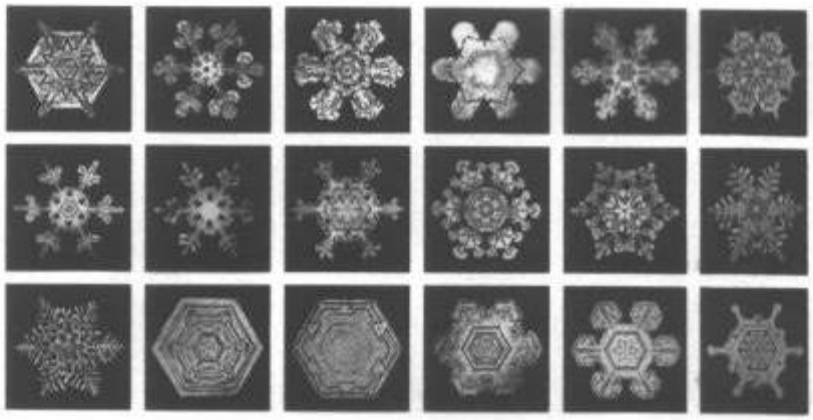

Examples of typical forms of snowflakes. Note that the scales for different pictures are different.

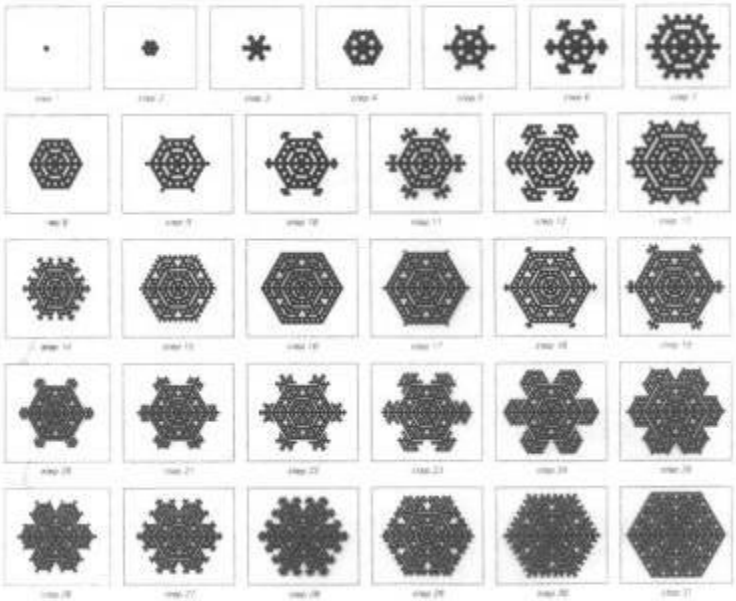

The evolution of a cellular automaton in which each cell on a hexagonal grid becomes black wherever exactly one of its neighbors was black on the step before. This rule captures the basic growth inhibition effect that occurs in snowflakes. The resulting patterns obtained at different steps look remarkably similar to many real snowflakes.

Näide 7. Taimed

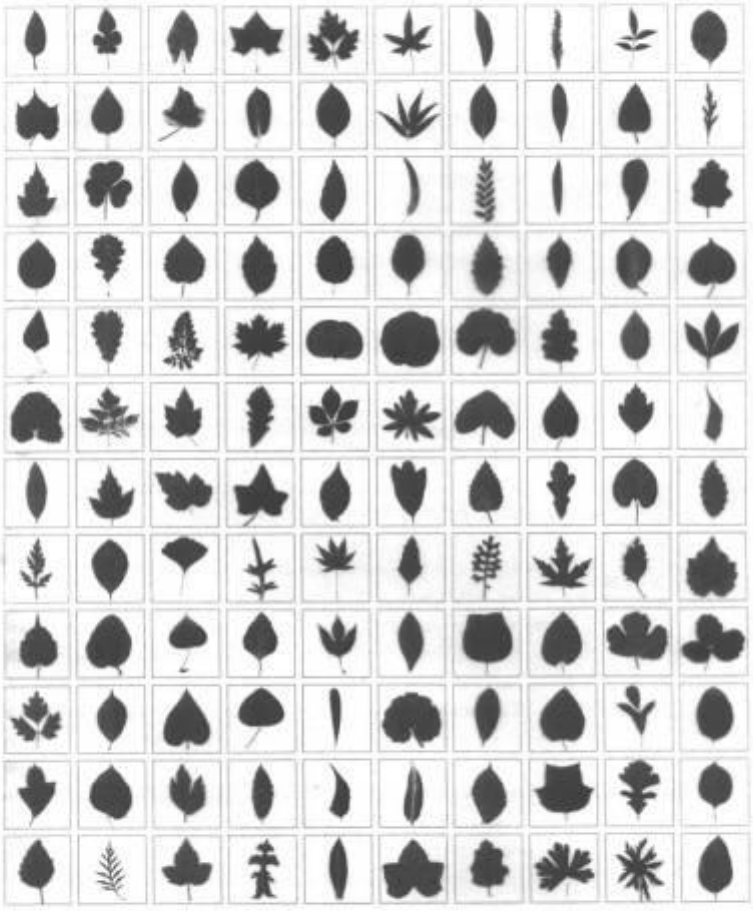

Examples of different kinds of leaves, mostly from common flowering plants. The diversity of shapes is remarkable, as is the similarity to the forms shown on the facing page. The leaves range in size from under an inch to many feet.

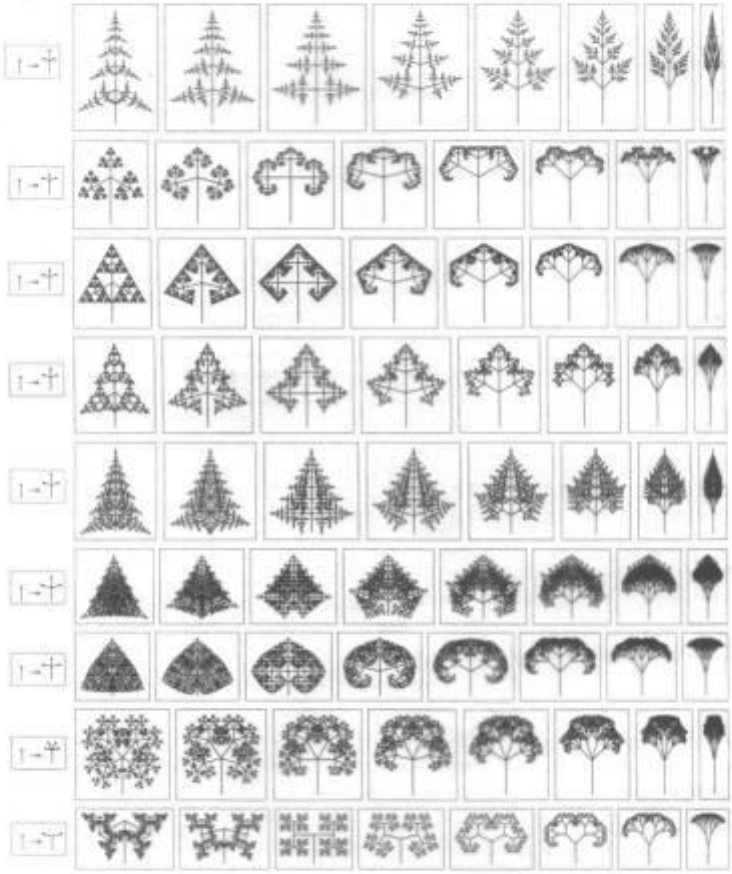

Limiting patterns produced by substitution systems of the type shown in the previous picture. The patterns on each row are obtained from rules that are set up to give branches with particular relative lengths. The angles between the branches are taken to increase by 15° in successive pictures across the row. Note that pictures shown on different rows are scaled differently—so that the initial vertical stem does not always appear with the same height. The similarity between pictures on this page and overall branching patterns and shapes of leaves in many kinds of plants is striking.